

This is the author's version of a paper that was later published as:

Frost, Ray and Martens, Wayde and Adebajo, Moses (2005) Synthesis of the mixed oxide catalysts based upon the nickel-copper hydrotalcites of the type  $\text{Ni}_x\text{Cu}_{6-x}\text{Cr}_2(\text{OH})_{16}(\text{CO}_3)_4\text{H}_2\text{O}$ . *Journal of thermal Analysis and calorimetry* 81(2):351-355.

Copyright 2005 Springer.

## SYNTHESIS OF THE MIXED OXIDE CATALYSTS BASED UPON THE NICKEL-COPPER HYDROTALCITES OF THE TYPE $\text{Ni}_x\text{Cu}_{6-x}\text{Cr}_2(\text{OH})_{16}(\text{CO}_3)_4\text{H}_2\text{O}$

R. L. Frost,\* W. N. Martens and M. O. Adebajo

*Inorganic Materials Research Program, School of Physical and Chemical Sciences,  
Queensland University of Technology, 2 George Street, Brisbane, GPO Box 2434,  
Queensland 4001, Australia.*

### Abstract

High resolution TG coupled to a gas evolution mass spectrometer has been used to study the thermal properties of a chromium based series of Ni/Cu hydrotalcites of formulae  $\text{Ni}_x\text{Cu}_{6-x}\text{Cr}_2(\text{OH})_{16}(\text{CO}_3)_4\text{H}_2\text{O}$  where  $x$  varied from 6 to 0. The effect of increased Cu composition results in the increase of the endotherms and mass loss steps to higher temperatures. Evolved gas mass spectrometry shows that water is lost in a number of steps and that the interlayer carbonate anion is lost simultaneously with hydroxyl units. Differential scanning calorimetry was used to determine the heat flow steps for the thermal decomposition of the synthetic hydrotalcites. Hydrotalcites in which  $\text{M}^{2+}$  consist of Cu, Ni or Co form important precursors for mixed metal-oxide catalysts. The application of these mixed metal oxides is in the wet catalytic oxidation of low concentrations of retractable organics in water. Therefore, the thermal behaviour of synthetic hydrotalcites,  $\text{Ni}_x\text{Cu}_{6-x}\text{Cr}_2(\text{OH})_{16}\text{CO}_3.n\text{H}_2\text{O}$  was studied by thermal analysis techniques in order to determine the correct temperatures for the synthesis of the mixed metal oxides.

**Keywords:** dehydration, dehydroxylation, hydrotalcite, differential scanning calorimetry, high-resolution thermogravimetric analysis

### Introduction

Much interest focuses on the use of nano-scale nickel oxide and copper oxide for catalyst use [1-7]. The copper oxide may be used as a solid solution or as a mixture of mixed oxides [8-12]. The application of these mixed oxides is in environmental applications such as the catalytic oxidation of carbon monoxide and the wet oxidation of organics in aqueous systems. It is apparent that such metal oxide mixtures may be obtained through the formation of hydrotalcites or double layered hydroxides. These nano-scale chemicals are produced through the thermal activation of copper salts such as copper carbonate, copper hydroxycarbonate either synthetic or natural (malachite) and other copper salts for example copper nitrate. Equally well the thermally activated copper oxide materials may be obtained from the

---

\* Author to whom correspondence should be addressed (r.frost@qut.edu.au)

thermal activation of copper based hydrotalcites. The activation of the copper and nickel oxides may be enhanced by a combination of the mixed oxides in specific ratios.

Hydrotalcites, or layered double hydroxides (LDH) are fundamentally anionic clays, and are less well-known but very much more diffuse in nature than cationic clays like smectites. The structure of hydrotalcite can be derived from a brucite structure ( $\text{Mg}(\text{OH})_2$ ) in which e.g.  $\text{Al}^{3+}$  or  $\text{Fe}^{3+}$  (pyroaurite-sjögrenite) substitutes a part of the  $\text{Mg}^{2+}$  [13, 14]. This substitution creates a positive layer charge on the hydroxide layers, which is compensated by interlayer anions or anionic complexes. In hydrotalcites a broad range of compositions are possible of the type  $[\text{M}^{2+}_{1-x}\text{M}^{3+}_x(\text{OH})_2][\text{A}^{n-}]_{x/n} \cdot y\text{H}_2\text{O}$ , where  $\text{M}^{2+}$  and  $\text{M}^{3+}$  are the di- and trivalent cations in the octahedral positions within the hydroxide layers with  $x$  normally between 0.17 and 0.33.  $\text{A}^{n-}$  is an exchangeable interlayer anion. In this research we are synthesizing mixed nickel-copper based hydrotalcites of the general formulae  $\text{Ni}_x\text{Cu}_{6-x}\text{Cr}_2(\text{OH})_{16}(\text{CO}_3) \cdot 4\text{H}_2\text{O}$  where  $x$  varies from 6 to 0. Whilst hydrotalcites based upon  $\text{Cu}_x\text{Mg}_{6-x}\text{Al}_2(\text{OH})_{16}(\text{CO}_3) \cdot 4\text{H}_2\text{O}$  have been studied [5, 15, 16], it is apparent that the Ni/Cu based hydrotalcites with Cr as the trivalent cation have not. Importantly, the use of hydrotalcites in the synthesis of nanocomposites has enabled high temperature phase composite materials to be manufactured. Important to this work is the knowledge of when the hydrotalcite decomposes and the mechanisms for this decomposition. This decomposition temperature influences the temperature of the formation of this nanocomposite such that might be used for the photo-oxidation of organics in aqueous systems. This research compliments our studies in the synthesis and characterization of hydrotalcites [17-22]. In this work we report the high-resolution thermogravimetric analysis of a series of hydrotalcites with different Cu and Ni ratios.

## Experimental

### Synthesis of hydrotalcite samples

The hydrotalcites were synthesised by the co-precipitation method. Hydrotalcites with a composition of  $\text{Ni}_x\text{Cu}_{6-x}\text{Cr}_2(\text{OH})_{16}(\text{CO}_3) \cdot 4\text{H}_2\text{O}$  and  $\text{Cu}_x\text{Ni}_{6-x}\text{Cr}_2(\text{OH})_{16}\text{CO}_3 \cdot n\text{H}_2\text{O}$  where  $x$  varied from 0 to 6, were synthesised. Two solutions were prepared, solution 1 contained 2M NaOH and 0.125M  $\text{Na}_2\text{CO}_3$ , solution 2 contained 0.75M  $\text{Cu}^{2+}$  ( $\text{Cu}(\text{NO}_3)_2 \cdot 6\text{H}_2\text{O}$ ) and 0.75M  $\text{Ni}^{2+}$  ( $\text{Ni}(\text{NO}_3)_2 \cdot 6\text{H}_2\text{O}$ ) (or 0.75M  $\text{Ni}^{2+}$  ( $\text{Ni}(\text{NO}_3)_2 \cdot 6\text{H}_2\text{O}$ ) together with 0.25M  $\text{Cr}^{3+}$  (as  $(\text{Cr}(\text{NO}_3)_3 \cdot 9\text{H}_2\text{O})$ ). Solution 2 in the appropriate ratio was added to solution 1 using a peristaltic pump at a rate of 40  $\text{cm}^3/\text{min}$ , under vigorous stirring, maintaining a pH of 10. To prepare hydrotalcites with different molecular formulae, the ratio of the  $\text{Ni}^{2+}/\text{Cu}^{2+}$  was varied according to the required formula. The precipitated minerals are washed at ambient temperatures thoroughly with water to remove any residual nitrate. The composition of the hydrotalcites was checked by ICP and ICP-AES analysis. The phase composition was checked by X-ray diffraction.

### Thermal Analysis

Thermal decomposition of the hydrotalcite was carried out in a TA high-resolution thermogravimetric analyzer (series Q500) in a flowing nitrogen atmosphere (80  $\text{cm}^3/\text{min}$ ). The samples were heated in an open platinum crucible at a rate of 2.0  $^\circ\text{C}/\text{min}$  up to 500 $^\circ\text{C}$ . The TGA instrument was coupled to a Balzers (Pfeiffer) mass spectrometer for gas analysis. Only selected gases were analyzed.

## Results and discussion

### *High Resolution Thermogravimetric Analysis*

Representative differential thermogravimetric analysis curves (DTG) of  $\text{Ni}_x\text{Cu}_{6-x}\text{Cr}_2(\text{OH})_{16}(\text{CO}_3)\cdot 4\text{H}_2\text{O}$  hydrotalcites and their mass spectrometric analysis curves of water and carbon dioxide are shown in Figures 1 and 2 respectively. The results of the integral of the DTG curves as determined by the band component analysis of the DTG curves are reported in Table 1. Each peak in the DTG curve represents a mass loss step and the total mass loss step is 100%. The results of the mass spectrometric analyses are provided in Table 2. The DTG curves are divided into mass loss steps according to the band component analysis. These steps correspond to the maxima in the DTG curves. The mass loss steps are further categorised according to the actual temperature of the mass loss.

The DTG pattern for the synthesized Ni/Cu/Cr hydrotalcites shows similarities except for the Cu/Cr hydrotalcite. The thermal analysis patterns show an initial mass loss from 50 to 100 °C with a second mass loss in the 142 to 240 °C (Table 1). This latter mass loss appears to be composed of overlapping mass loss steps. The Ni/Cr hydrotalcite shows two mass loss steps at 236 and 297.9 °C. A higher mass loss step at 357 °C is also identified. The  $\text{Cu}_2\text{Ni}_4$  hydrotalcite shows a single mass loss step at 229 °C. The  $\text{Cu}_3\text{Ni}_3$  chromium hydrotalcite has mass loss steps at 195, 239 and 289 °C. The  $\text{Cu}_2\text{Ni}_4$  hydrotalcite thermal analysis pattern shows two mass loss steps at 173, 212 and 243 °C. The thermal analysis pattern for the Cu chromium hydrotalcite appears different with mass loss steps observed at 142 °C, two minor mass loss steps at 170 and 197 °C and a further mass loss step at 390 °C.

The question arises as to why the thermal behaviour of the hydrotalcite series is different. In brucite type solids, there are tripod units  $\text{M}_3\text{OH}$  with several metal cations such as M, M', M''. In hydrotalcites such as those based upon Ni and Cu of formula  $\text{Ni}_x\text{Cu}_{6-x}\text{Cr}_2(\text{OH})_{16}(\text{CO}_3)\cdot 4\text{H}_2\text{O}$ , a number of statistical permutations of the  $\text{M}_3\text{OH}$  units are involved. These are  $\text{Cu}_3\text{OH}$ ,  $\text{Ni}_3\text{OH}$ ,  $\text{Cr}_3\text{OH}$  and combinations such as  $\text{Cu}_2\text{NiOH}$ ,  $\text{Ni}_2\text{CuOH}$ ,  $\text{Cu}_2\text{CrOH}$ ,  $\text{Cr}_2\text{CuOH}$ ,  $\text{Cr}_2\text{NiOH}$ ,  $\text{Ni}_2\text{CrOH}$ , and even  $\text{CuNiCrOH}$ . These types of units will be distributed according to a probability distribution according to the composition. In this model, a number of assumptions are made, namely that the molecular assembly is random and that no islands or lakes of cations are formed. Such assembly is beyond the scope of this work but needs to be thoroughly investigated. In the simplest case namely  $\text{Ni}_6\text{Cr}_2(\text{OH})_{16}(\text{CO}_3)\cdot 4\text{H}_2\text{O}$  the types of units would be  $\text{Ni}_3\text{OH}$ ,  $\text{Ni}_2\text{CrOH}$ ,  $\text{NiCr}_2\text{OH}$  and  $\text{Cr}_3\text{OH}$ . A similar situation would exist for the  $\text{Cu}_6\text{Cr}_2(\text{OH})_{16}(\text{CO}_3)\cdot 4\text{H}_2\text{O}$  hydrotalcite. In a somewhat oversimplified model, for the  $\text{Cu}_6\text{Cr}_2(\text{OH})_{16}(\text{CO}_3)\cdot 4\text{H}_2\text{O}$  hydrotalcite, the principal dehydroxylation mass loss steps could be attributed to the  $\text{Cu}_3\text{OH}$  and  $\text{Cr}_3\text{OH}$  units. It is possible that the dehydroxylation steps are cation dependent based on the hydrogen bond strength of the cationic OH unit.

For the  $\text{Ni}_6\text{Cr}_2(\text{OH})_{16}(\text{CO}_3)\cdot 4\text{H}_2\text{O}$  hydrotalcite, there are four principal mass loss steps which may be assigned to (a) loss of water in the 75 to 100 °C temperature range (b) loss of hydroxyls from the  $\text{Cu}_3\text{OH}$  and  $\text{Cr}_3\text{OH}$  units as well as the mixed cationic species (c) loss of carbonate and water simultaneously and (d) loss of carbonate only. For this hydrotalcite the loss of the hydroxyl units occurs over a very sharp temperature range namely 122 to 156°C. The theoretical mass losses for the  $\text{Ni}_6\text{Cr}_2(\text{OH})_{16}(\text{CO}_3)\cdot 4\text{H}_2\text{O}$  hydrotalcite are 31.62 % for dehydroxylation, 6.97 % for the loss of carbon dioxide and 8.37 % for dehydration. The observed mass loss steps for the dehydration step are 13 %, for the dehydroxylation 19.9 %

and for loss of carbon dioxide is 6.3 %. There are considerable differences between the predicted and observed values. The significance of this result means that the mass losses for these hydrotalcites are due to the loss of water and carbon dioxide simultaneously.

The mass loss steps for the Ni/Cr hydrotalcite are observed at 236, 298 and 357 °C with % mass losses of 16.6, 20.7 % and 17.7 %. For the Ni<sub>4</sub>Cu<sub>2</sub>/Cr hydrotalcite a broad mass loss step is observed centered upon 229 °C. This mass loss step accounts for 90.7 % of the mass loss. For the Ni<sub>3</sub>Cu<sub>3</sub>/Cr hydrotalcite three resolvable steps are observed at 195, 239 and 289 °C with percentage mass loss steps of 29.0, 47.4 and 13.6 %. For the Ni<sub>2</sub>Cu<sub>4</sub>/Cr hydrotalcite a similar set of values is obtained with mass loss steps observed at 174, 212 and 243 °C. It is proposed that the observation of the two additional steps may be attributed to the loss of hydroxyl units from the different cations in the structure. If this is the case then thermal analysis is providing specific information on the arrangement of the hydroxyl units. It is possible the cations are not randomly distributed but are forming lakes of cations in the structure.

### ***Mass spectrometric analysis***

The mass spectrometric analysis of the evolved gases is shown in Figure 2. The results of the analyses are reported in Table 2. Two gases are monitored namely water and carbon dioxide. The mass spectrometric curves of evolved gases namely water vapour and carbon dioxide are also shown in Figure 2. The figure clearly shows the MS of the evolved gases as a function of temperature. What may be clearly distinguished is that (a) initially water vapour is measured only (b) there is a temperature range where the evolved gases are water vapour and carbon dioxide and (c) a temperature interval over which carbon dioxide is evolved only. The mass spectra were analysed by band resolution on the assumption that the total mass is 100% for each of water vapour and carbon dioxide. The results are reported in Table 2. The MS of nitric oxide and nitrogen dioxide, the possible by-products of the thermal decomposition of nitrate was also measured but no mass spectrum was obtained, thus indicating the absence of nitrate in the interlayer space. The fundamental principle that the addition of the mass spectrometric curves follows the DTG curve with absolute precision. This means that a direct comparison can be made between the DTG results and the mass spectrometric results.

The Ni<sub>4</sub>Cu<sub>2</sub>Cr<sub>2</sub>(OH)<sub>16</sub>(CO<sub>3</sub>).4H<sub>2</sub>O hydrotalcite mass spectrum shows the loss of water in five steps at temperatures of 103, 205, 239, 324 and 393 °C. The evolved mass of water at 103 °C is 9.5 % of total water mass. This corresponds to the dehydration of the hydrotalcite. The value of 9.5% agrees well with the theoretical value of 8.27 % for the hydrotalcite water content. The evolved water vapour observed at 205 and 239 °C with mass losses of 21.7 and 27.7 % must correspond to the dehydroxylation of the hydrotalcite. Dehydroxylation appears to take place in steps with a continuous loss over the 300 to 400 °C temperature range. In comparison the evolved carbon dioxide comes off in three stages at 218, 259 and 424 °C. The % of evolved carbon dioxide in these three steps is 45.5, 51.3 and 3.1 %. The carbon dioxide is lost in two main steps and corresponds with the mass loss dehydroxylation steps 2 and 3. Thus the dehydroxylation and loss of carbonate occur over similar temperature ranges. This fact supports the concept that the carbonate is bonded to the hydroxyl units after the dehydration. It is envisaged that carbonate would be bonded to the different types of hydroxyl units as indicated above. It is the strength of the hydrogen bond formed between the carbonate and the hydroxyl unit which determines the temperature for the loss of carbonate

and the dehydroxylation. The observation of carbon dioxide at 424.3 °C is attributed to the formation of metal carbonates in the thermal analysis and their decomposition occurs at a higher temperature.

The mass spectra of evolved water vapour and carbon dioxide for the  $\text{Ni}_3\text{Cu}_3\text{Cr}_2(\text{OH})_{16}(\text{CO}_3)\cdot 4\text{H}_2\text{O}$  hydrotalcite strongly resembles that of the  $\text{Ni}_4\text{Cu}_2\text{Cr}_2(\text{OH})_{16}(\text{CO}_3)\cdot 4\text{H}_2\text{O}$  hydrotalcite. The evolved water vapour appears at 102, 179, 217 and 335 °C. The first mass loss step corresponds to the dehydration of the hydrotalcite with a relative mass of 17.0 %. The next three steps correspond to the dehydroxylation of the hydrotalcite with mass steps of 28.5, 46.5 and 8.0 %. The evolved carbon dioxide appears in two mass loss steps at 249 and 300 °C. Just as for the  $\text{Ni}_4\text{Cu}_2\text{Cr}_2(\text{OH})_{16}(\text{CO}_3)\cdot 4\text{H}_2\text{O}$  hydrotalcite, the observation of the evolved carbon dioxide appears at higher temperatures than that for the evolved water vapour. This seems to indicate that the dehydroxylation is taking place before the loss of carbonate. For the  $\text{Ni}_2\text{Cu}_4\text{Cr}_2(\text{OH})_{16}(\text{CO}_3)\cdot 4\text{H}_2\text{O}$  hydrotalcite, the evolved water vapour appears over four steps at 90, 175, 212 and 363 °C. The relative % masses for these steps are 23.7, 29.4, 31.6 and 15.2 %. The first step corresponds to dehydration and the high value observed simply means the sample contained adsorbed water which is not unexpected. As for the  $\text{Ni}_3\text{Cu}_3$  hydrotalcite the evolved carbon dioxide occurs in two steps at 199 and 251 °C with relative mass of 28.7 and 71.3 %.

The mass loss of water for the  $\text{Cu}_6\text{Cr}_2(\text{OH})_{16}(\text{CO}_3)\cdot 4\text{H}_2\text{O}$  hydrotalcite at 135 °C is 30.7% which may be compared with the mass loss step of 26.5% for the DTG step at 143.5°C. It must be kept in mind that the precision of the DTG results will be significantly greater than that obtained by the MS results. Similarly the mass loss step at 165 °C of 5.6% may be compared with the mass loss of 7.6% at 163 °C in the MS data. The mass loss step 5 at 190°C for this hydrotalcite must be compared with the sum of the evolved masses of both water and carbon dioxide. The mass gain of carbon dioxide at 387 °C is directly comparable to the mass loss step 7. In this step  $\text{CO}_2$  is being evolved only. These results prove that there is excellent correspondence between the mass loss steps and the mass gain of evolved gases.

There is an apparent trend in the dehydration temperature as the Ni is replaced by the Cu in the  $\text{Ni}_x\text{Cu}_{6-x}\text{Cr}_2(\text{OH})_{16}(\text{CO}_3)\cdot 4\text{H}_2\text{O}$  hydrotalcites. The temperature of dehydration decreases as the moles of  $\text{Cu}^{2+}$  increases. A similar trend is observed for the dehydroxylation of the hydrotalcites. The temperature of decarbonation also follows a similar trend although the variation is not as pronounced.

## Conclusions

Thermal analysis defines the temperature to which hydrotalcites must be heated to form the mixed metal oxides. A series of  $(\text{Ni}_x\text{Cu}_{6-x})\text{Cr}_2(\text{OH})_{16}(\text{CO}_3)\cdot 4\text{H}_2\text{O}$  hydrotalcites with copper substitution for nickel have been studied by a combination of differential scanning calorimetry and high resolution thermogravimetry in combination with an evolved gas mass spectrometer. High resolution DTGA combined with mass spectrometry shows that the temperatures of the dehydroxylation and dehydration of the  $(\text{Ni}_x\text{Cu}_{6-x})\text{Cr}_2(\text{OH})_{16}(\text{CO}_3)\cdot 4\text{H}_2\text{O}$  hydrotalcite decreases with increased Cu composition. Three principal mass loss steps are observed (a) loss of adsorbed water in the 90 to 110°C temperature range (b) dehydroxylation in the 200 to 248°C (d) loss of carbonate in the 200 to 350°C temperature range. Thermal analysis defines the temperature to which the hydrotalcite must be heated to form the mixed metal oxides. This temperature is a function of the composition of the hydrotalcite.

Importantly the synthesis of mixed Ni/Cu hydrotalcites and their decomposition enables the formation of mixed metal oxides which are mixed at the atomic level rather than at a particle level. These mixed metal oxides are then suitable for use as catalysts such as in the photocatalytic oxidation of recalcitrant organics in water.

## References

1. M. D. Arco, V. Rives and R. Trujillano, *Stud. Surf. Sci. Catal.* 87 (1994) 507.
2. C. Barriga, J. M. Fernandez, M. A. Ulibarri, F. M. Labajos and V. Rives, *J. Solid State Chem.* 124 (1996) 205.
3. O. Clause, M. Gazzano, F. Trifiro, A. Vaccari and L. Zatorski, *Appl. Catal.* 73 (1991) 217.
4. O. Clause, B. Rebours, E. Merlen, F. Trifiro and A. Vaccari, *J. Catal.* 133 (1992) 231.
5. F. Kovanda, K. Jiratova, J. Rymes and D. Kolousek, *Appl. Clay Sci.* 18 (2001) 71.
6. F. M. Labajos and V. Rives, *Inorg. Chem.* 35 (1996) 5313.
7. P. Porta and S. Morpurgo, *Appl. Clay Sci.* 10 (1995) 31.
8. K. K. Rao, M. Gravelle, J. S. Valente and F. Figueras, *J. Catal.* 173 (1998) 115.
9. V. Rives, A. Dubey and S. Kannan, *Phys. Chem. Chem. Phys.* 3 (2001) 4826.
10. V. Subramani, S. Hashimoto, N. Satoh, K. Suzuki and T. Mori, *Prepr. - Am. Chem. Soc., Div. Pet. Chem.* 46 (2001) 17.
11. E. H. Van Broekhoven, in *Eur. Pat. Appl.*, (AKZO N. V., Neth.). Ep, 1988, p. 16 pp.
12. S. Velu, K. Suzuki, S. Hashimoto, N. Satoh, F. Ohashi and S. Tomura, *J. Mater. Chem.* 11 (2001) 2049.
13. L. Hickey, J. T. Klopogge and R. L. Frost, *J. Mater. Sci.* 35 (2000) 4347.
14. J. Theo Klopogge and R. L. Frost, *Phys. Chem. Chem. Phys.* 1 (1999) 1641.
15. E. Kanezaki, K. Kinugawa and Y. Ishikawa, *Chem. Phys. Lett.* 226 (1994) 325.
16. Y. Kobayashi, T. Honna, T. Katamoto and A. Yamamoto, in *Jpn. Kokai Tokkyo Koho*, (Toda Kogyo Corp., Japan). Jp, 2000, p. 8 pp.
17. R. L. Frost, W. Martens, Z. Ding and J. T. Klopogge, *J. Therm. Anal. Calorim.* 71 (2003) 429.
18. R. L. Frost and K. L. Erickson, *J. Therm. Anal. Calorim.* 78 (2004) 367.
19. R. L. Frost and K. L. Erickson, *J. Therm. Anal. Calorim.* 76 (2004) 217.
20. R. L. Frost, Z. Ding and H. D. Ruan, *J. Therm. Anal. Calorim.* 71 (2003) 783.
21. E. Horvath, J. Kristof, R. L. Frost, N. Heider and V. Vagvoelgyi, *J. Therm. Anal. Calorim.* 78 (2004) 687.
22. R. L. Frost, M. L. Weier and K. L. Erickson, *J. Therm. Anal. Calorim.* 76 (2004) 1025.

## List of Tables

**Table 1. Results of the DTG for Ni/Cu /Cr hydrotalcites.**

**Table 2. Results of the MS for Ni/Cu /Cr hydrotalcites**

**Table 1. Results of the DTG for Ni/Cu/Cr hydrotalcites.**

<b>Ni/Cu/Cr Hydrotalcites</b>	<b>Ni/Cu 6:0 Temp/ % Mass loss</b>	<b>Ni/Cu 4:2 Temp/ % Mass loss</b>	<b>Ni/Cu 3:3 Temp/ % Mass loss</b>	<b>Ni/Cu 2:4 Temp/ % Mass loss</b>	<b>Ni/Cu 0:6 Temp/ % Mass loss</b>
Mass Loss Step 1		88 4.0		88 16.6	
Mass Loss Step 2		106 2.6	102 9.38		142 60.3
Mass Loss Step 3			195 29.0	174 22.8	170 5.6
Mass Loss Step 4	236 16.6	229 90.7	239 47.4	212 30.2	197 23.7
Mass Loss Step 5	298 20.7		289 13.6	243 30.45	
Mass Loss Step 6	357 17.7	451 2.7	471 0.5	460 0.32	388 10.0

**Table 2. Results of the MS for Ni/Cu/Cr hydrotalcites.**

Ni/Cu /Cr Hydrotalcites	Ni/Cu 6:0		Ni/Cu 4:2		Ni/Cu 3:3		Ni/Cu 2:4		Ni/Cu 0:6	
	Temp/ % Mass Loss		Temp/ % Mass Loss		Temp/ % Mass Loss		Temp/ % Mass Loss		Temp/ % Mass Loss	
	H <sub>2</sub> O	CO <sub>2</sub>	H <sub>2</sub> O	CO <sub>2</sub>	H <sub>2</sub> O	CO <sub>2</sub>	H <sub>2</sub> O	CO <sub>2</sub>	H <sub>2</sub> O	CO <sub>2</sub>
Mass Loss Step 1	134.5 30.7		102.7 9.5		101.6 17.0		89.7 23.7		75.5 4.0	
Mass Loss Step 2	212 17.6		204.9 21.7	217.6 45.5	178.9 28.5		174.9 29.4	198.9 28.7	111.8 23.7	
Mass Loss Step 3	258 7.6		238.7 27.7	258.7 51.3	216.7 46.5	248.9 73.1	212.2 31.6	251.2 71.3	205.6 39.0	205.9 7.3
Mass Loss Step 4	188.0 32.1	216 61.3	323.9 25.7	424.3 3.1	334.7 8.0	299.5 26.8	362.9 15.2		248.8 33.2	269.5 92.6
Mass Loss Step 5	307.4 11.9	387.0 38.0	393.3 15.3							



## List of Figures

**Figure 1 Differential mass loss of the hydrotalcites**

$(\text{Ni}_x\text{Cu}_{6-x})\text{Cr}_2(\text{OH})_{16}(\text{CO}_3)\cdot 4\text{H}_2\text{O}$  as (a)  $x=6$  (b) 4 (c) 3 (d) 2 (e) 0.

**Figure 2 MS of water and carbon dioxide for the hydrotalcites**

$(\text{Ni}_x\text{Cu}_{6-x})\text{Cr}_2(\text{OH})_{16}(\text{CO}_3)\cdot 4\text{H}_2\text{O}$  as (a)  $x=6$  (b) 4 (c) 3 (d) 2 (e) 0.

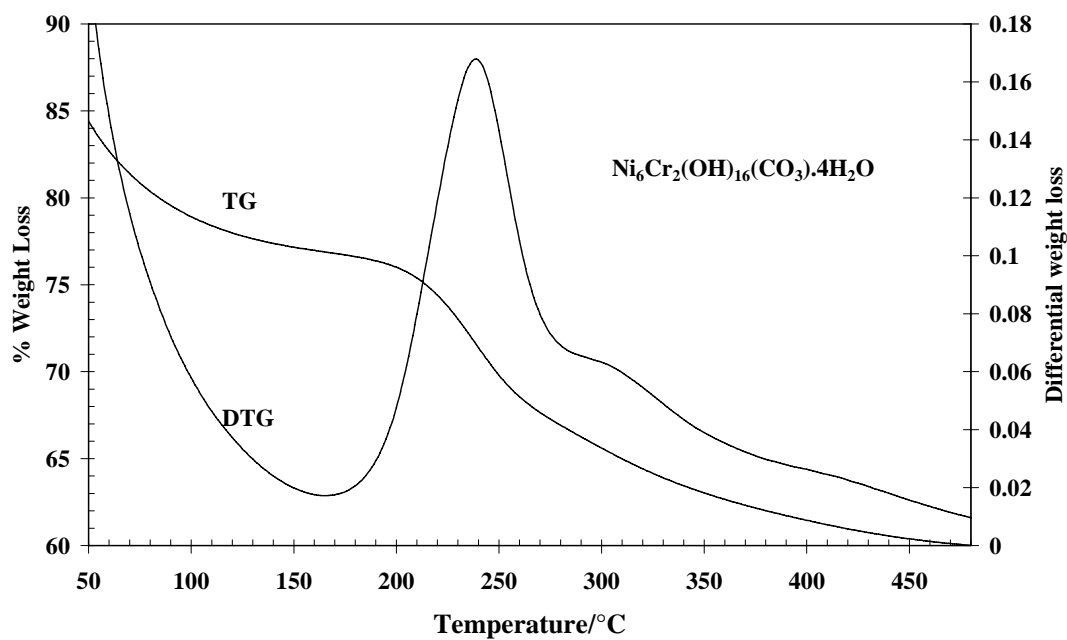


**Figure 1a**

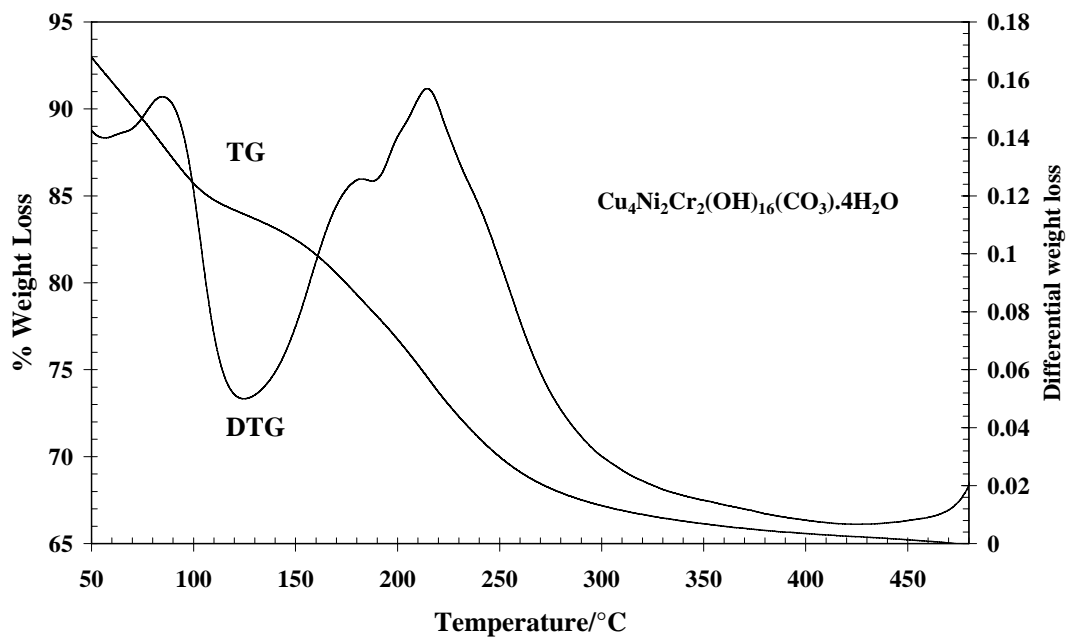


Figure 1b

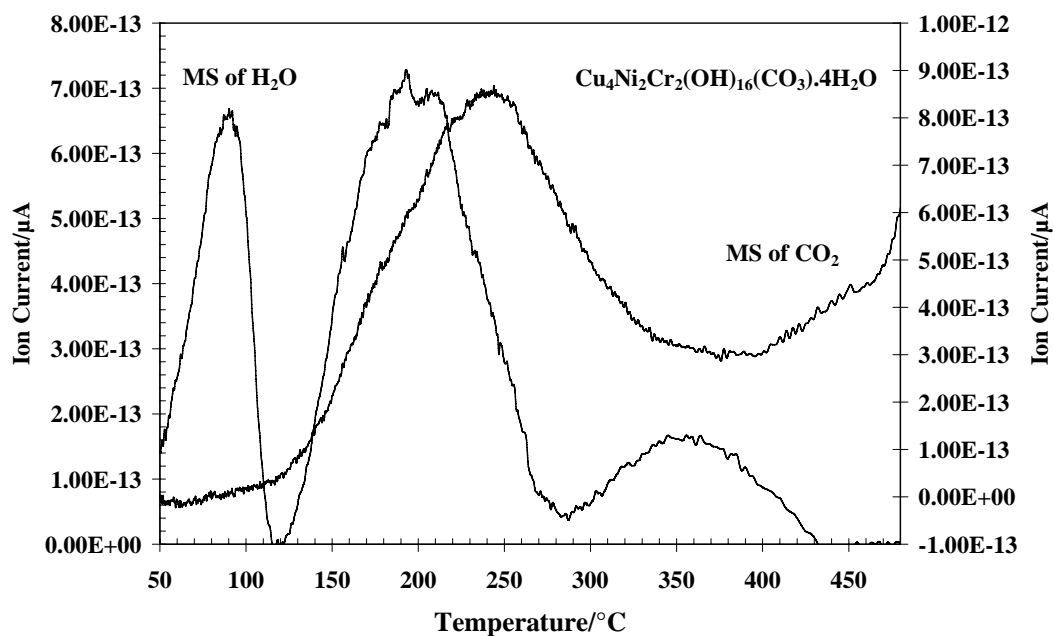


Figure 2